Zircon concentrate analysis for sixteen rare earth elements by the complex of nuclear analytical methods

I. Silachyov[1] ○

Abstract

Two samples of zircon concentrate by local manufacturers were investigated for the first time for their rare earth elements (REE) content by instrumental neutron activation analysis (INAA) and energy dispersive X-ray fluorescence analysis. Comparator variant of INAA based on an external standard (Fe) and two internal standards (Th, La) was used to determine the elements divided into three groups depending on the detector type, radionuclide half-lives, and suitable comparator.
High Y and heavy REE contents of the samples exceeding their crustal averages up to two orders of magnitude confirmed significance of the zircon concentrate as an important source of these elements production as a by-product.

Keywords Zircon concentrate · Rare earth elements · Neutron activation analysis · X-ray fluorescence

Introduction

Due to the sweeping upgrowth of modern technologies over the last three decades, rare earth elements (REE), including all lanthanides (except for radioactive Pm which is extremely rare in the Earth's crust), Y, and Sc fast became crucially important in different industrial sectors for a variety of applications [1–3]. Ever-growing REE consumption had to resort both to search and exploration of their new traditional (natural) resources and to utilization of the alternative non-traditional sources of these elements. Apart from recycling of the served out industrial products, the latter include different wastes (red mud, phosphogypsum, coal combustion fly ash, mining and industrial residues [1, 4–6]), as well as by-products of phosphate, kaolin and some other productions [7–9]. Thumping majority of the various REE sources exploited today are substantially more prevalent in light rare earth elements (LREE) while the demand pattern has changed recently towards more intense use of far less abundant heavy REE (HREE) [10]. So, great interest grew of late years in this connection in the widespread zircon mineral (ZrSiO₄) as a unique primary [11] and secondary (different

ore beneficiation tailing) [12, 13] source of Y and heavy lanthanides.

Main difficulty of zircon analysis for REE contents by the most up-to date plasma-based analytical techniques such as inductively coupled plasma optical emission spectrometry and mass spectrometry (ICP-OES and ICP-MS) consists in extreme chemical resistance of this mineral [14, 15]. Zircon is not practically dissolved by mineral acids, so multistage procedures including alkaline or carbonate fusion are usually applied for its decomposition [16]; however, complete dissolution can hardly be achieved [17]. The other drawbacks of REE analysis by these methods are rather traditional ones mainly consisting in appreciable matrix effect and significant spectral (ICP-OES), isobaric, polyatomic, and ionization interferences (ICP-MS) caused by matrix components [18].

Laser ablation-inductively coupled-plasma mass spectrometry (LA-ICP-MS) allows avoiding complex and time-consuming wet-chemical digestion but in the case of local analysis of separate mineral grains only. To implement bulk investigations, heterogeneity of laser-ablation targets is tided over by pressing of powder pellets or fusion glasses production [19]. The first method requires intensive grinding of refractory minerals such as zircon to achieve powder dimensions < 5 μm that is much smaller standard requirements to conduct element analysis (76 μm or 200 mesh). Then, even a binder is not used, the whole process suffers from the risk of contamination from grinding reagents and abrasion of milling equipment. Moreover, the "nugget effect" from

✉ I. Silachyov
silachyov@inp.kz

[1] Institute of Nuclear Physics, Ibragimov, Str.1,
050032 Almaty, Republic of Kazakhstan

zircon is not still overcome after rock thorough grinding up to 1 µm of the particles. These drawbacks are kept out of by the flux-free fusion method [20], but other ones appear. Some problems may be ignored in the case of REE determination (highly volatile element loss), but how to melt completely the refractory minerals in rocks is still "a question of interest" [19]. On the other hand, LA-ICP-MS method still suffers from interferences, sensitivity drift and elemental/isotopic fractionation [21], hence to obtain reliable quantitative data rigorous and suitable calibration methods should be applied.

The other nondestructive analytical techniques such as X-ray fluorescence analysis (XRF) and instrumental neutron activation analysis (INAA) seem more dependable than LA-ICP-MS for zircon element content investigation. Owing to a large sample area (about 1 cm^2), characteristic X-ray fluorescence is detected from, as well as to the known peculiarities of INAA, heterogeneity of zircon grains distribution doesn't matter and the standard sample treatment can be carried out.

Main restriction of the modern commercially available energy dispersive (ED) X-ray spectrometers to determine REE is caused by X-ray tubes they are equipped with. Since maximum 50 kV of high voltage are usually applied to them, only the first four light lanthanides may be determined by K-series, even if an intermediate target is not used. The same lanthanides are generally accessed when characteristic X-ray radiation of a sample is excited by a suitable radionuclide source (^{241}Am) [22]. Both variants are of minor interest in elemental analysis of zircon samples enriched by HREE, so EDXRF in this case finds only its traditional application [23].

Due to their much better resolution in the low-energy part of spectra, wave dispersive (WD) X-ray spectrometers can be applied to analyze all lanthanides by their L-series, at least in principle [24]. However, this still remains a challenge when real rocks are investigated since numerous lanthanides L-lines can't be totally resolved overlapping one with another and with K-lines of matrix elements. Larger efforts including accurate calibration and sophisticated algorithms to overcome influence of spectral interferences should be applied [25], so WDXRF method seems being deprived of a clear advantage over LA-ICP-MS. More often it is used in addition to the latter to find major element contents while trace elements (including REE) are determined by LA-ICP-MS from the same fused samples [20].

In spite of the keen rivalry from the up-to-date analytical techniques, INAA still occupies a leading position in rock analysis for REE content [26]. Its most important advantages comprise high sensitivity, minimum matrix effects, absence of the reagent blank, and usually slight spectral interferences. The main drawbacks of INAA are long time of REE determination and nuclear reactor inaccessibility from time to time.

INAA is probably the most appropriate method to analyze REE in the zircon bulk samples [27]. High content of Zr reaching 49.5 wt% in a pure mineral doesn't practically present trouble owing to its very low thermal neutron cross-section. However, considerable isomorphic impurities (up to several wt%) of Hf may be a certain problem resulting in deterioration of sensitivity of all element analysis. Additional inconvenience is caused by rather high content of U impeding determination of light REE due to their production by U fission. Similar difficulties have been overcome once studying REE composition of Zr and Ta–Zr–Nb ore samples [28].

In the present work, comparator INAA [29] was tested to analyze almost all rare earth elements (except for Y and Pm) by their long-lived and short-lived radionuclides in two samples of zircon concentrates by different industrial manufacturers. Y content of the samples, because of its very low value of the thermal neutrons cross-section [30], was found by EDXRF.

Experimental

One of the analyzed samples (sample 1) is presented by a certified reference material (CRM) of zircon concentrate GSO4087, trademark КЦЗ, produced by the Institute of Reference Materials, Ekaterinburg, Russian Federation. The original product was manufactured by a Russian ore mining-and-processing enterprise according to the performance specification TU 14–10–015–98. The other sample (sample 2) is an analogous product specimen of the concentrating mill of the ilmenite deposit Shokash, Republic of Kazakhstan. Table 1 presents major oxide contents of the samples. All the values are certified in sample 1 with the exception of HfO$_2$ determined by INAA. Approximate composition of sample 2 by ICP-OES (without confidence limits) is taken from [31].

Since dimensions of sample 2 grains didn't meet the requirements of element analysis it was additionally ground and passed through a FRITSCH Gmbh (Germany) sieve with mesh size 0.071 mm.

Table 1 Major oxides contents of zircon concentrate samples, wt%

Compound	Sample 1	Sample 2
ZrO$_2$	65.9 ± 0.2	61.9
SiO$_2$	32.3 ± 0.1	32.1
Al$_2$O$_3$	1.16 ± 0.02	1.51
Fe$_2$O$_3$	0.081 ± 0.004	0.11
TiO$_2$	0.163 ± 0.007	0.99
HfO$_2$	1.14 ± 0.10	1.18

To avoid over-irradiation (due to high Hf contents) during INAA carrying out assay masses of the analyzed samples and corresponding irradiation times were estimated empirically beforehand. About 10 mg for the long-time irradiation and about 100 mg for the short-time one were sealed in flat double polyethylene bags. Assay mass was deliberately diminished in the first case to reduce self-absorption of some low-energy analytical gamma-rays by the rather heavy matrix. During short-time irradiation self-absorption can be neglected since the energy of the selected analytical gamma-lines exceeds 300 keV (see below). There wasn't need for the special monitor of the neutron flux (ZrO_2 [28]) since any of the analyzed samples can be used so.

The smaller bags were wrapped into aluminium foil and irradiated in the position № 4 inside the peripheral vertical channel № 10–6 of the light-water research reactor WWR-K, the Institute of Nuclear Physics (INP), Almaty, for 1.5 h by the thermal neutron (< 0.625 eV) and fast neutron (0.1–1.15 MeV) flux density about $8.9 \cdot 10^{13}$ cm^{-2} s^{-1} and $6.0 \cdot 10^{12}$ cm^{-2} s^{-1}, respectively [32]. The larger bags were fixed inside HDPE transport capsules across the neutron flux to minimize its gradient effect and irradiated for 3 min by the thermal neutron flux density approximately $5 \cdot 10^{12}$ cm^{-2} s^{-1} with the help of an automated pneumatic transport system [33]. Its irradiation terminal is installed in a "dry" horizontal channel of WWR-K close to the outer side of the tank. The samples are thus activated by a more thermalized neutron flux comparing with the vertical peripheral irradiation channels within the reactor's active zone.

According to preliminary investigations, two types of the semiconductor detectors to perform gamma-spectrometric measurements, as well as the corresponding sets of analyzed elements and the used comparators, were selected. Most measurements, both by the long-lived radionuclides (to determine La, Yb, Lu, U, Sc, Tb, Tm, and Th – the first group of elements) and the short-lived ones (Pr, Eu, Dy, Er – the second group), were carried out by an extended-range HPGe coaxial detector GX5019 (Canberra) with a relative efficiency of 50% and an energy resolution of 1.86 keV at the 1332 keV peak of ^{60}Co connected to a multi-channel analyzer DSA-1000. The in-house software developed at INP to provide gamma-spectrometric analysis was applied for spectra collection. A special assay of 10.0 ± 0.1 mg of iron powder (CRM GSO1634, the Institute of Reference Materials, Ekaterinburg, Russian Federation, 98.2 ± 0.1 wt% Fe) irradiated together with the studied samples was used as the comparator to analyze the first group of the elements by their long-lived radionuclides. To avoid difficulties resulting from the differences of counting geometries and analyzer dead time, the method of the "external addition" of the comparator was applied [34], i.e. an analyzed sample and Fe comparator were measured simultaneously placed one beside another. Iron

mass in the 10 mg samples of zircon concentrate doesn't exceed 0.008 mg (Table 1) and is negligible comparing to the Fe comparator mass. First counting (to define La, Yb, Lu, and U content) took place for 30 min after 7 days of decay, the next – for 1 h after 3 weeks; the distance from the samples to the detector cap was 60 mm and 24 mm, respectively.

To analyze remaining lanthanides by their long-lived radionuclides (Sm, Ho, Nd, Gd, and Ce – the third group) much better energy resolution is necessary due to a high spectral background under their low-energy analytical gamma-lines caused by the Compton continuum from intensive high-energy gamma-lines of ^{95}Zr, ^{175}Hf, and ^{181}Hf. That is why a planar HPGe detector GLP36360 with the crystal dimensions 36×13 mm and an energy resolution of 585 eV at the 122 keV peak of ^{57}Co connected to a multi-channel analyzer DSPEC LF, both by ORTEC, was used. MAESTRO software was applied for spectra collection which happened thrice: after 6 days of decay (for 40 min, to determine Sm and Ho), after 2 weeks (for 2 h, Nd and the second measurement to determine Ho), and after 6 weeks (for 16 h, Ce, Gd). Such a long last decay time is necessary to make ^{239}Np X-ray K$_{\alpha1}$ peak (103.37 keV) and ^{153}Sm gamma-line (103.18 keV) completely decayed as a serious spectral interference for Gd determination (see below). The distance from the samples to the detector cap was 40 mm for the first counting and 10 mm for the second and the third ones. Th was used as the internal comparator in this case with its mass fraction determined with the help of the GX5019 detector.

Eu content of the samples was found by its short-lived radionuclide ^{152m}Eu (together with Dy, Er, and Pr contents) since sensitivity and accuracy turned up better than by the long-lived ^{152}Eu. The same coaxial detector was used in this case. Counting time and geometry were defined by sensitivity of ^{142}Pr determination being the worst of the four. To reduce spectral background caused by some intensive gamma-lines – ^{165}Dy (half-life is 2.3 h), ^{97}Nb (1.2 h), ^{56}Mn (2.6 h), the decay time was brought to several hours. The samples were taken out of the capsules, placed at the distances of 24 mm to the detector cap and counted for 2.5 h. Likewise above, La determined before was used as the internal comparator.

Both detectors were calibrated for relative detection efficiency $\varepsilon(E)$, where E is a gamma-ray energy, with the help of a multi-gamma ray standard MGS-1 (^{152}Eu, ^{154}Eu, ^{155}Eu) and an isotopic source ^{133}Ba, both by Canberra. The latter was used to extend the low-energy range of the planar detector. The calibration curves were fitted with fourth power polynomials.

Basic principles of gamma-ray spectra treatment to calculate analytical peak count rates have been mentioned earlier [34]. "AnalGamma" software also developed at INP was used for spectra treatment.

Table 2 presents main nuclear parameters of the analytical gamma-lines of the radionuclides used to determine REE content of zircon concentrate samples as well as accounted interferences depending on the detector type. If more than one line can be used for analysis preference was usually given to higher energy lines in order to diminish gamma-ray self-absorption by rather heavy matrix. However, Sm was analyzed by a softer gamma-line to avoid severe spectral interferences from ^{239}Np and ^{233}Pa radionuclides. The same concerns Nd determination but in this case because of a very low detection efficiency of ^{147}Nd high-energy gamma-line (531.02 keV) with the planar detector. Despite its low quantum yield, the high-energy line of ^{165}Dy was selected owing to its quite sufficient count rate (high Dy content). The part of ^{177}Lu count rate resulted from ^{176}Yb by the (n, γ) reaction was evaluated considering the Yb to Lu average crustal ratio [28]. ^{176}Yb contribution to ^{177}Lu activity after 1.5 h of irradiation is no more than 1.7% and can be neglected. The interferences coinciding with the analyzed radionuclides – uranium fission products (^{140}La and others) are denoted as U(n, f). The spectral superposition caused by ^{133}Xe also produced by fission of uranium contained in the samples was accounted using the expression below. Other possible interferences in ZrO$_2$–SiO$_2$ matrix were considered insignificant and hence ignored.

Since ^{166}Ho and ^{133}Xe gamma-lines can't be reliably resolved by the GLP36360 detector, count rate of the former $J_{Ho}(t_1)$ to determine its content in the samples was calculated as follows solving the system of two decay equations:

$$J_{Ho}(t_1) = \frac{J_{\Sigma}(t_2)/k - J_{\Sigma}(t_1)\exp(-\lambda_2(t_2 - t_1))}{\exp(-\lambda_{Ho}(t_2 - t_1)) - \exp(-\lambda_{Xe}(t_2 - t_1))}, \qquad (1)$$

where $J_{\Sigma}(t)$ is the sum peak count rate, λ_{Ho} and λ_{Xe} are decay constants of ^{166}Ho and ^{133}Xe, t_1 and t_2 are the decay times of the first and of the second counting, respectively, and factor k takes account of different measuring geometries.

To evaluate contribution coefficients F_{Ui} of uranium fission products to analyze La, Ce, and Nd contents, a CRM of uranium ion solution (Perkin Elmer) was used. The values of F_{Ui} were assessed empirically as the ratios of the count rates of the analytical gamma-lines of the corresponding radionuclide to the count rate of ^{239}Np under the same counting conditions.

Yttrium content of the zircon concentrate samples was determined with a portable energy dispersive X-ray spectrometer RLP-21 T by LLP "AspapGeo" (Almaty, Kazakhstan) designed to study element composition of powdered samples of rocks, minerals, ores, and concentrates. Elemental contents are calculated using a high-effective reference-free modified method of fundamental parameters. The accuracy of the RLP-21 T algorithm of spectra treatment was repeatedly confirmed with the help of different CRMs during its routine exploitation. That is why the spectrometer is applied as a rule to measure Fe or other element contents

Table 2 Main nuclear parameters and interferences of the radionuclides used to determine REE contents of zircon concentrate samples by comparator INAA

Radionuclide	Half-life, days	Energy, keV	Quantum yield, %	Interferences	Energy, keV	Quantum yield, %	Detector
^{46}Sc	83.8	889.28	99.98	–	–	–	GX5019
^{140}La	1.68	1596.2	95.4	U(n, f)	–	–	GX5019
^{141}Ce	32.5	145.44	48.3	U(n, f) ^{175}Yb	– 144.86	– 0.67	GLP36360
^{142}Pr	19.1 h	1575.6	3.7	–	–	–	GX5019
^{147}Nd	11.0	91.11	28.1	U(n, f)	–	–	GLP36360
^{153}Sm	1.94	69.67	4.73	–	–	–	GLP36360
^{152m}Eu	9.3 h	963.39	11.7	^{152m}Eu	961.06	0.12	GX5019
^{153}Gd	240.4	103.18	21.1	^{233}Pa (^{233}Th)	103.86	0.854	GLP36360
^{160}Tb	72.3	298.58	26.1	^{233}Pa	298.81	0.088	GX5019
^{165}Dy	2.3 h	361.68	0.904	–	–	–	GX5019
^{166}Ho	1.12	80.57	6.71	^{133}Xe	81.00	36.9	GLP36360
^{171}Er	7.5 h	308.29	64.0	–	–	–	GX5019
^{170}Tm	128.6	84.25	2.48	^{182}Ta	84.68	2.65	GX5019
^{175}Yb	4.18	396.33	13.2	–	–	–	GX5019
^{177}Lu	6.65	208.37	10.4	^{176}Yb → ^{177}Lu	208.37	10.4	GX5019
^{233}Pa (^{233}Th)	27.0	311.90	38.5	–	–	–	GX5019 GLP36360
^{239}Np (^{239}U)	2.36	277.60	14.4	–	–	–	GX5019

of geological samples used as the internal standard in comparator INAA [29, 33]. RLP-21 T is enrolled in the State Register of Measuring Devices (Certificate № 670, valid to 27.07.2025), and the corresponding analytical technique is registered by the National Body for Certification of Kazakhstan (Certificate № 69–2022, valid to 15.02.2027).

Layout of zircon concentrate analysis by two nuclear analytical methods can be presented on the whole as Fig. 1 shows. The comparators used to determine mass fraction of certain groups of elements are marked in bold.

REE content calculation by INAA

Element contents C_a (ppm) of the analyzed samples were calculated according to the next equation of simple comparator method of standardization in INAA [35] using the internal standard method [29] (lower case indices a and c mean an analyzed element and the comparator, respectively):

$$C_a = C_c \frac{k_{0,c} J_a \varepsilon(E_c)(f + Q_0^c)(SDC)_c G_c F_c}{k_{0,a} J_c \varepsilon(E_a)(f + Q_0^a)(SDC)_a G_a F_a} K_{a,c}, \qquad (2)$$

where C_c is the element comparator content of the sample (ppm), k_0 is k_0-factor relatively to 411.8 keV gamma-line of radionuclide ^{198}Au for the gamma-lines of the comparator and the analyzed element [30], J is net peak count rate of the analytical gamma-line of the corresponding radionuclide (cps), Q_0 is the resonance integral I_0 (cm^2) to the thermal neutron cross-section σ_0 (cm^2) ratio, f is the thermal to epithermal neutron flux ratio, $S = 1 - \exp(-\lambda t_{irr})$ is saturation factor, $D = \exp(-\lambda t_d)$ is decay factor, $C = (1 - \exp(-\lambda t_m))/\lambda t_m$ is the counting factor (t_{irr}, t_d, and t_m are irradiation, decay and measuring time), G is the correction factor for neutron self-shielding by the sample, F is the correction factor for analytical gamma-ray self-absorption in the sample.
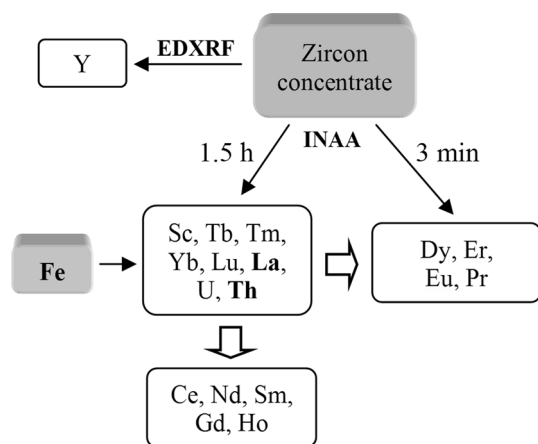

Fig. 1 Layout of samples analysis by EDXRF and INAA

Due to very low zirconium σ_0 value G factor for the zircon concentrate samples smaller than 100 mg of the mass is very close to unity like for common rocks with low contents of elements with anomalously high σ_0 values.

Self-absorption of different energy gamma-rays in the samples was evaluated in the approximation of a thin irradiating layer [36]. Maximum correction amounting to 6.5% was introduced for ^{153}Sm analytical gamma-line (69.67 keV). If a gamma-ray energy exceeds 300 keV, F factor becomes < 1% and the corresponding correction was not accounted for.

Coefficient $K_{a,c}$ introduced in [29] compensates for an analytical bias which may be caused by various reasons such as the absence of Q_0 correction for the deviation of thermal neutron flux from 1/E law and others. $K_{a,c}$ values once estimated empirically by the repeated irradiation and counting of different multi-element CRMs in the same geometry remain invariable during the whole time of detector exploitation. The coefficients also enable evade some intricate items such as count rate correction for true coincidences.

The model resonance to thermal neutron flux ratio 1/f was evaluated by the "bare bi-isotopic method" [37] using the analyzed zircon concentrate samples as the monitors of the neutron flux spectral composition as was mentioned above. The corresponding expression was presented earlier more than once [28, 33, 34]. In this investigation 1/f value in the irradiation position was 0.0292 ± 0.006.

Results and discussion

Accuracy of REE determination in rock CRMs by the internal standard based comparator INAA was repeatedly verified by the author [28, 29]. The studied samples are characterized by uranium high contents reaching first hundreds ppm as XRF preliminarily showed. That is why several relevant rock CRMs certified for REE content were additionally selected and analyzed. They are: OREAS 100a and OREAS 101b by Ore Research & Exploration (Australia), and OSO 528 by the All-Russian Scientific Research Institute of Mineral Resources (Moscow). The first two CRM represent uranium-bearing ores, the third one represents a phosphorous REE uranium ore. Such objects are usually enriched with heavy rare earth elements compared to common rocks or other types of REE ores. The CRM samples were prepared, irradiated and analyzed as described above, i.e. using the definite comparators for concentration standardization, each for a certain group of the elements as Fig. 1 shows. To avoid over-irradiation, the CRM assay mass was diminished to 50 mg with irradiation time coming to 2.5 h. All CRMs were measured only once.

The ratios of uranium content to light lanthanides contents in three CRM were 0.50–0.85 for La, approximately

0.29–0.48 for Ce, and about 1 for Nd. Then contribution of the uranium fission products to the count rates of the corresponding analytical gamma-lines was found rather reasonable – less than 1.5% for [140]La, 10–13% for [141]Ce, and 20–24% for [147]Nd. Such a small correction to [140]La count rate despite high U/La ratio makes possible to use lanthanum content reliably as an internal comparator to analyze some other REE (see Fig. 1).

The ratios of uranium to holmium contents are far more dramatic reaching 28.1 for OREAS 100a, 62.5 for OREAS 101b, and 20.3 for OSO 528. In this case ^{133}Xe contribution to the area of unresolved double peak [166]Ho + [133]Xe came up to approximately 59%, 78%, and 42%, respectively, after 6 days of the decay time.

As for the other spectral interferences presented in Table 2, only Ta contribution to Tm analytical gamma-line count rate is significant reaching approximately 19% in OREAS 100a and 14% in OREAS 101b. Remaining interferences were resolved by the spectra treatment software or neglected.

The common expression used to estimate expanded uncertainty $U(C_a)$ of determination of the first group of elements by comparator INAA is the following ($P = 0.95$):

$$U(C_a) \approx 2C_a \sqrt{\frac{u(J_a)^2}{J_a^2} + \frac{u(J_c)^2}{J_c^2} + \frac{u(C_c)^2}{C_c^2} + \delta_a^2 + \frac{u(M)^2}{M^2} + \frac{u(m_c)^2}{m_c^2}},$$ (3)

where $u(J_a)$, $u(J_c)$, and $u(C_c)$ are standard uncertainties of the corresponding values as in Eq. (2), δ_a is relative standard uncertainty of element analysis by comparator INAA (methodical uncertainty), $u(M)$ is standard uncertainty of the sample mass M, and $u(m_c)$ is the same for comparator mass m (all the ratios and δ_a are in %). The latter two terms were introduced into Eq. (3) due to external concentration standardization that was used; they are about 1% each. Relative uncertainty of Fe content of the comparator (CRM GSO1634) is about 0.1%, i.e. negligible. The term of δ_a assessed earlier with the help of the CRMs seems being the main component of $U(C_a)$. Its values range from 2.2% (La determination) to 3.4% (determination of Tm).

When Eq. (3) is used to estimate expanded uncertainty of the other two groups of element analysis by the internal standard based comparator INAA, uncertainty of mass determination does not apply (see Eq. (2)) and the corresponding term is omitted.

The results of CRM analyses for fifteen rare earth elements by comparator INAA, for Y content by XRF, as well as for U and Th contents as the main interfering elements (also by INAA) are demonstrated in Tables 3, 4 and 5. Both certified and measured values are presented together with their 95% confidence limits, absence of the latter means an indicative value, and dash (-) means that

Table 3 REE, Th, and U contents of CRM OREAS 100a in ppm ($P = 0.95$)

Element	Certified value	Measured value	E_n-score
Sc	6.10	6.68 ± 0.50	–
Y	142 ± 3	132 ± 23	− 0.43
La	260 ± 9	264 ± 25	0.15
Ce	463 ± 20	460 ± 45	− 0.06
Pr	47.1 ± 2.4	47.6 ± 5.7	0.08
Nd	152 ± 8	145 ± 14	− 0.43
Sm	23.6 ± 0.4	24.0 ± 2.3	0.17
Eu	3.71 ± 0.23	3.64 ± 0.43	− 0.14
Gd	23.6 ± 1.4	23.6 ± 3.0	0
Tb	3.80 ± 0.23	3.71 ± 0.32	− 0.23
Dy	23.2 ± 0.4	23.7 ± 2.8	0.18
Ho	4.81 ± 0.14	4.89 ± 0.45	0.17
Er	14.9 ± 0.5	15.4 ± 1.9	0.25
Tm	2.31 ± 0.11	2.33 ± 0.21	0.08
Yb	14.9 ± 0.4	15.7 ± 1.3	0.59
Lu	2.26 ± 0.11	2.30 ± 0.20	0.18
Th	51.6 ± 2.7	50.7 ± 4.2	− 0.18
U	135 ± 7	126 ± 10	− 0.74

Table 4 REE, Th, and U contents of CRM OREAS 101b in ppm ($P = 0.95$)

Element	Certified value	Measured value	En-score
Sc	8.70	9.17 ± 0.78	–
Y	178 ± 9	164 ± 23	− 0.57
La	789 ± 40	804 ± 76	0.17
Ce	1331 ± 67	1324 ± 150	− 0.04
Pr	127 ± 7	127 ± 15	0.00
Nd	378 ± 19	394 ± 40	0.36
Sm	48 ± 3	48.5 ± 4.6	0.09
Eu	7.77 ± 0.39	8.02 ± 0.96	0.24
Gd	41 ± 2	40.1 ± 5.0	− 0.17
Tb	5.37 ± 0.27	5.54 ± 0.53	0.29
Dy	32.1 ± 1.6	34.2 ± 4.1	0.48
Ho	6.34 ± 0.31	6.28 ± 0.62	− 0.09
Er	18.7 ± 0.9	18.8 ± 2.3	0.05
Tm	2.66 ± 0.14	2.67 ± 0.26	0.03
Yb	17.6 ± 0.9	18.3 ± 1.7	0.36
Lu	2.58 ± 0.13	2.64 ± 0.25	0.21
Th	37.1 ± 1.9	37.2 ± 3.5	0.03
U	396 ± 20	387 ± 38	− 0.21

the element content was not assessed at all. E_n-score values taking into account the expanded uncertainty of both certified values and the measured results are presented too as a criterion recommended by IUPAC to verify laboratory performance [38].

Table 5 REE, Th, and U contents of CRM OSO 528 in ppm ($P = 0.95$)

Element	Certified value	Measured value	En-score
Sc	15.7 ± 1.5	16.8 ± 1.5	0.52
Y	603 ± 59	595 ± 100	− 0.07
La	444 ± 33	446 ± 42	0.04
Ce	782 ± 69	765 ± 78	− 0.16
Pr	87 ± 3.4	89 ± 10	0.20
Nd	382 ± 26	376 ± 38	− 0.13
Sm	82.1 ± 4.0	83.4 ± 8.0	0.15
Eu	21.7 ± 0.5	21.6 ± 2.5	− 0.04
Gd	100 ± 6	102 ± 13	0.13
Tb	15.1 ± 0.4	14.4 ± 1.3	− 0.51
Dy	89.7 ± 3.2	88.6 ± 9.5	− 0.11
Ho	18.5 ± 0.7	18.7 ± 1.9	0.10
Er	51.2 ± 0.9	50.6 ± 6.1	− 0.10
Tm	6.68 ± 0.3	6.40 ± 0.60	− 0.42
Yb	40.2 ± 0.6	41.0 ± 3.8	0.21
Lu	5.64 ± 0.23	5.83 ± 0.54	0.32
Th	–	9.33 ± 0.80	–
U	376 ± 13	361 ± 34	− 0.41

It's important to note that the measured mass fractions of La and Th which were used as the internal standards agree with their certified values within ≤ 2% of relative bias. Contents of the other REE and U differ from their certified values by no more than 10%, which has been accepted as an admissible deviation. Along with the absolute values of E_n-score which appeared less than unity this implies that the results of rare earth elements determination in the CRMs can be considered acceptable by this criterion.

On the other hand, paying attention to the industrial significance of the study, the assessed values of $U(C_a)$ presented in Tables 3, 4 and 5 were compared with the corresponding ones of the allowable standard deviation of the results of these element routine determination recommended by a branch standard (mineral resources exploration) [39]. Accuracy of the analysis proved to meet the requirements in all the cases with the exception of U higher contents (OREAS 101b, OSO 528), but uranium determination is not the main aim of the investigation.

Thus, it has been demonstrated that determination of sixteen REE is feasible by the above approach, i.e. basically by comparator INAA, using Fe as an external comparator, and then some of the analyzed elements as the internal standards to find contents of the others.

To analyze two zircon concentrate samples for the mass fractions of the fifteen REE by comparator INAA, twelve gamma-ray spectra were recorded using two types of detectors after different decay times. Several fragments of the most informative gamma-ray spectra of sample 1 are presented in Figs. 2 and 3 in a log-linear scale; spectra of sample 2 are analogous. Figure 2 displays the spectrum collected by the coaxial detector to measure mass fractions of the four lanthanides by their short-lived radionuclides. It was recorded after 4 h of accumulation to gain necessary statistics of ^{142}Pr net peak count rate. Two parts of interest including analytical gamma-lines of these radionuclides and that of ^{140}La internal standard are adduced in different scales. Several hours of the decay of the most short-lived radionuclides ^{56}Mn and ^{165}Dy advantaged reducing analyzer dead time.

Figure 3 demonstrates a low-energy part of the gamma-ray spectrum collected by the planar detector for two hours after 2 weeks of decay to determine Nd and Ho (second measurement) contents. Due to its high mass fraction ^{175}Yb still presents a considerable spectral interference for ^{141}Ce, so the latter was analyzed much later. Despite sharp decrease of the GLP36360 detection efficiency with gamma-ray energy, count rate of the 311.9 keV gamma-line of ^{233}Pa is
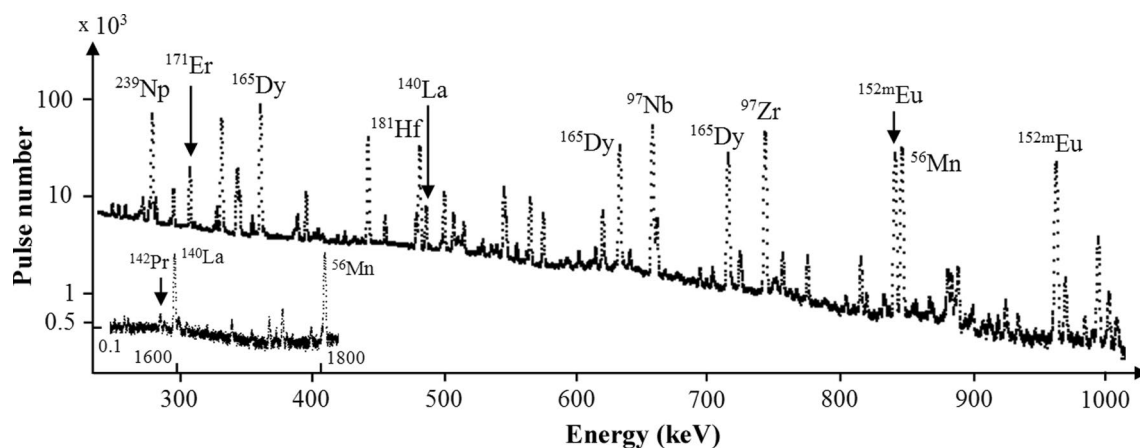
Fig. 2 Part of the gamma-ray spectra of sample 1 (GSO4087) counted by GX5019 after 2.5 h of decay (in a log-linear scale)
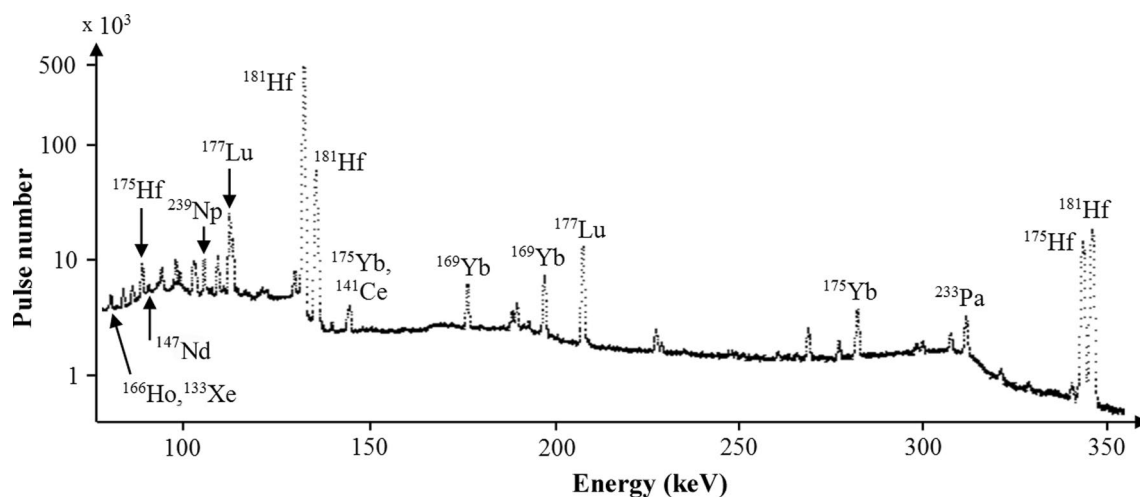
Fig. 3 Part of the gamma-ray spectra of sample 1 (GSO4087) counted by GLP36360 after 2 weeks of decay (in a log-linear scale)

Table 6 REE, Th, and U contents of two zircon concentrate samples in ppm ($P = 0.95$)

Element	Sample 1	Sample 2
Sc	69.9 ± 5.2	80.6 ± 6.0
Y	920 ± 100	1110 ± 200
La	56.8 ± 4.3	26.7 ± 2.0
Ce	186 ± 22	50 ± 9
Pr	16.1 ± 1.9	7 ± 1
Nd	76 ± 14	43 ± 9
Sm	23.4 ± 2.3	13.5 ± 1.4
Eu	3.91 ± 0.40	3.33 ± 0.35
Gd	36 ± 8	35 ± 8
Tb	11.9 ± 0.8	10.7 ± 0.8
Dy	104 ± 12	132 ± 16
Ho	37.3 ± 4.2	38.0 ± 4.6
Er	162 ± 19	223 ± 26
Tm	30.2 ± 2.2	34.6 ± 2.5
Yb	282 ± 21	398 ± 30
Lu	55.9 ± 4.2	81.2 ± 6.1
Th	129 ± 9	167 ± 12
U	189 ± 15	328 ± 25

sufficient to use it as an internal standard. Intensive gamma-lines of the abundant and strongly activated two Hf isotopes induce high count rate of the Compton background substantially restricting sensitivity of the analysis.

Results of all rare earth elements, Th and U determination in the zircon concentrate samples are presented in Table 6. The values of the expanded uncertainty of Y content determination are ensured by the certified analytical technique; for the other elements they are assessed according to Eq. (3). Main spectral interferences are caused by the high U

contents. Contribution of the uranium fission products to the count rate of La analytical gamma-line is not too considerable reaching about 7% (sample 1) and 25% (sample 2). The situation is more dramatic in the case of Ce and Nd analysis. Corrections to ^{141}Ce gamma-line intensity amounted approximately 26% and 65%, and 43% and 66% to that of ^{147}Nd. Nevertheless, these values are distinctly lower than the 90% contribution of the uranium fission products assessed earlier [40] as the approximate limit of quantitative analysis (30% of the expanded uncertainty).

Owing to rather high Ho contents and short decay time (6 days) contribution of ^{133}Xe to the unresolved integral peak was only about 22% and 32% for samples 1 and 2, respectively, i.e. lower than could be expected. Another peculiarity is the absence of usual corrections to ^{170}Tm analytical gamma-line caused by ^{182}Ta due to lack of tantalum after chemical treatment of raw material. There were no any other significant spectral interferences as well. However, the low count rate of ^{142}Pr and ^{153}Gd gamma-lines together with very unfavorable peak-to-background ratio of the latter decreased substantially accuracy of the analysis. That is why Gd mass fractions of the samples can be regarded rather as information values only.

As Table 6 shows, lanthanides contents with even atomic numbers (Ce, Nd, Sm, Gd, Dy, Er, Yb) are higher than contents of their adjacent lighter and heavier neighbors with odd atomic numbers that is in compliance with the Oddo-Harkins rule for the majority of natural REE. I.e. initial raw material benefication didn't result in redistribution of REE interrelation. On the whole, zircon concentrate samples demonstrate the same sharp disproportion of HREE (Gd–Lu) to LREE (La–Eu) contents, typical of zircon mineral. Yttrium group elements (Y and HREE) contain 79 wt% (sample 1) and 90 wt% (sample 2) of the sum REE quantity. The most

Fig. 4 REE mass fractions of two zircon concentrate samples relatively to their corresponding average UCC contents
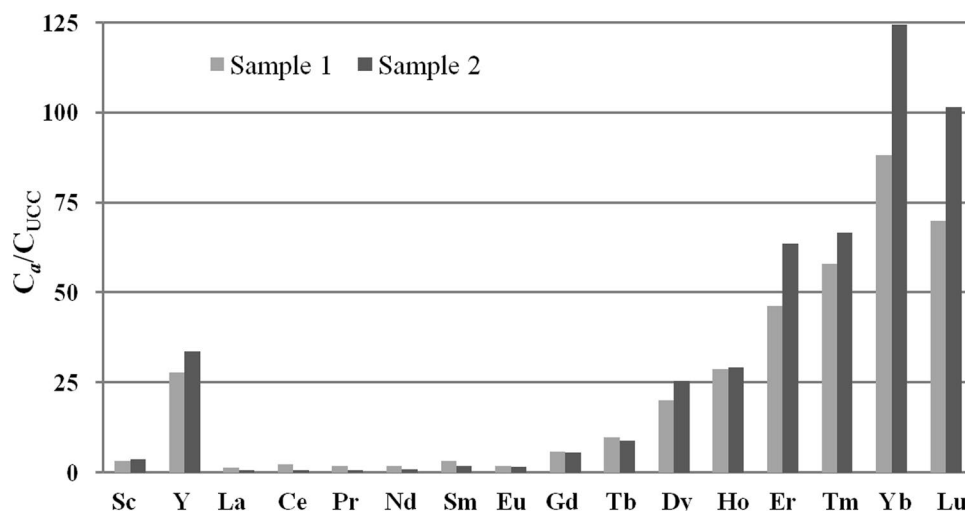
demonstrative pattern appears if REE mass fractions are expressed in relative units C_a/C_{UCC}, where C_{UCC} are the corresponding average contents of the upper continental crust (UCC) [41]. Y and some HREE contents of the zircon concentrate samples exceed their crust averages by several tens. This ratio can reach two orders of magnitude and even more for the heaviest rare earth elements (Fig. 4). The obtained result numerically demonstrates industrial significance of zircon concentrate of different origin as an important source of valuable heavy rare earth elements.

Conclusions

A complex of nuclear analytical methods mainly presented by INAA and supplemented by XRF, previously applied successfully to analyze geological samples for REE contents, was tested for the same purpose with a more complicated object – a zircon concentrate characterized by a heavy artificial matrix. The comparator variant of INAA based both on an external and two internal standards was used for concentration standardization since the relative method could be scarcely applicable in this case. Taking account of the intensive background, element ratios and some spectral interferences, REE were divided into three groups to analyze in similar conditions with the help of two different types detectors. An external Fe comparator was applied to find mass fraction of the first group elements including the two used afterwards as the internal standards (Th and La). Special efforts were exerted to determine the elements analyzed by their short-lived radionuclides such as Dy, Er, Pr. The result of sixteen REE contents can be considered as an essential enough since it could be hardly obtained by other up-to-date methods due to extreme chemical resistance of zircon.

Both available zircon concentrate samples confirmed high mass fractions of Y and valuable HREE exceeding their

average UCC contents by up to two orders of magnitude. The author hopes this can incite local producer to develop technologies of HREE extraction from zircon concentrate as a by-product before its utilization for other purpose.

References

1. Dushyantha N, Batapola N, Ilankoon IMSK et al (2020) The story of rare earth elements (REEs): occurrences, global distribution, genesis, geology, mineralogy and global production. Ore Geol Rev. https://doi.org/10.1016/j.oregeorev.2020.103521
2. Balaram V (2019) Rare earth elements—a review of applications, occurrence, exploration, analysis, recycling, and environmental impact. Geosci Front 10:1285–1303
3. Zhou B, Li Z, Chen C (2017) Global potential of rare earth resources and rare earth demand from clean technologies. Minerals. https://doi.org/10.3390/min7110203
4. Costis S, Mueller KK, Coudert L et al (2021) Recovery potential of rare earth elements from mining and industrial residues—a review and cases studies. J Geochem Explor. https://doi.org/10.1016/j.gexplo.2020.106699
5. Zhang W, Noble A, Yang X et al (2020) A comprehensive review of rare earth elements recovery from coal-related materials. Minerals. https://doi.org/10.3390/min10050451
6. Rychkov VN, Kirillov EV, Kirillov SV et al (2018) Recovery of rare earth elements from phosphogypsum. J Cleaner Prod 196:674–681
7. Peiravi M, Dehghani F, Ackah L et al (2021) A review of rare-earth elements extraction with emphasis on non-conventional sources: Coal and coal byproducts, iron ore tailings, apatite, and phosphate byproducts. Min, Metall Explor 38(1):1–26
8. Alves FE, Neumann R, Ávila CA et al (2021) Mineralogical auditing of the volta grande mine (SE Brazil) Sn–Ta–Nb–Li processing plant, aiming at REE recovery as by-products. Appl Earth Sci 130:198–208

9. Dehaine Q, Filippov LO, Joussemet R (2017) Rare earths (La, Ce, Nd) and rare metals (Sn, Nb, W) as by-products of kaolin production – Part 2: Gravity processing of micaceous residues. Miner Eng 100:200–210

10. Paulick H, Machacek E (2017) The global rare earth element exploration boom: an analysis of resources outside of China and discussion of development perspectives. Resour Policy 52:134–153

11. Makeyev AB, Skublov SG (2016) Y-REE-rich zircons of the Timan region: geochemistry and economic significance. Geochem Int 54(9):788–794

12. Trisnawati I, Prameswara G, Mulyono P et al (2020) Sulfuric acid leaching of heavy rare earth elements (HREEs) from Indonesian zircon tailing. Int J Technol 11(4):804–816

13. Handini T (2020) Separation the zircon mineral from tailing tin mining using shaking table. J Phys Conf Ser. https://doi.org/10.1088/1742-6596/1436/1/012127

14. Singh A, Padmasubashini V, Gopal L (2012) Determination of uranium, thorium and rare-earth elements in zircon samples using ICP-MS. J Radioanal Nucl Chem 294:19–25

15. Krishnakumar M, Chakrapani G, Satyanarayana K et al (2016) Selective matrix removal and ICP-OES determination of trace uranium, rare earth elements and yttrium in zircon minerals. J Radioanal Nucl Chem 307:497–505

16. Zhang J, Wang L, Jiang D (2012) Decomposition process of zircon sand concentrate with CaO–NaOH. Rare Met 31(4):410–414

17. Thibault Y, Gamage McEvoy J, Duguay D (2020) Optimizing Zr and REE recovery from zircon through a better understanding of the mechanisms governing its decomposition in alkali media. In: Azimi G (ed) Rare metal technology. Springer, Cham

18. Zuma MC, Lakkakula J, Mketo N (2022) Recent trends in sample preparation methods and plasma-based spectrometric techniques for the determination of rare earth elements in geological and fossil fuel samples. Appl Spectrosc Rev 57:353–377

19. Zhang W, Hu Z (2019) Recent advances in sample preparation methods for elemental and isotopic analysis of geological samples. Spectroch Acta, Part B. https://doi.org/10.1016/j.sab.2019.105690

20. Tamura A, Akizawa N, Otsuka R et al (2015) Measurement of whole-rock trace-element composition by flux-free fused glass and LA-ICP-MS: evaluation of simple and rapid routine work. Geochem J 49:243–258

21. Lin J, Liu Y, Yang Y et al (2016) Calibration and correction of LA-ICP-MS and LA-MC-ICP-MS analyses for element contents and isotopic ratios. Solid Earth Sci 1:5–27

22. Karivai A, Zuzaan P, Gustova V (2011) A method for the determination of some rare earth elements and their correlation with thorium using X-ray fluorescence. Phys Part Nucl Lett 6(8):576–580

23. Siyanbola WO, Fasasi AY, Funtua II et al (2005) Energy dispersive X-ray fluorescence analysis of samples of the Nigerian zircons. Nucl Instrum Methods Phys Res, Sect B 239:426–432

24. Schramm R (2016) Use of X-ray fluorescence analysis for the determination of rare earth elements. Phys Sci Rev. https://doi.org/10.1515/psr-2016-0061

25. Smoliński A, Stempin M, Howaniec N (2016) Determination of rare earth elements in combustion ashes from selected Polish coal mines by wavelength dispersive X-ray fluorescence spectrometry. Spectroch Acta, Part B 116:63–74

26. Stosch H-G (2016) Neutron activation analysis of the rare earth elements (REE) – with emphasis on geological materials. Phys Sci Rev. https://doi.org/10.1515/psr-2016-0062

27. Attallah MF, Hilal MA, Moussa SI (2017) Quantification of some elements of nuclear and industrial interest from zircon mineral using neutron activation analysis and passive gamma-ray spectroscopy. Appl Radiat Isot 128:224–230

28. Silachyov IYu (2020) Neutron activation analysis of rare earth raw material using a planar detector and thorium as an internal standard. Int J Biol Chem 13:117–129

29. Silachyov I (2016) Rare earths analysis of rock samples by instrumental neutron activation analysis, internal standard method. J Radioanal Nucl Chem 310:573–582

30. K0-Neutron activation analysis link page. The NDC k0-databaze 2019. http://www.kayzero.com/k0naa/k0naaorg/Links.html. Accessed 15 Feb 2023

31. Simonov YA, Kritskii AA, Tomashov VA et al (2009) Study of the process of MgO regeneration from products of its sintering with zircon. Russ J Non-ferrous Metals 50(5):457–460

32. Koltochnik SN, Sairanbayev DS, Chekushina LV et al (2018) Comparison of neutron spectrum in the WWR-K reactor with LEU fuel against HEU one. NNC RK Bulletin 76(4):14–17 (**(in Russian)**)

33. Silachyov IYu (2021) Determination of indium in its ore resources by comparator neutron activation analysis. Int J Biol Chem 14:106–116

34. Silachyov I (2020) Elemental analysis of vegetation samples by INAA internal standard method. J Radioanal Nucl Chem 324:97–108

35. Hamidatou L, Slamene H, Akhal T, Zouranen B (2013) Concepts, instrumentation and techniques of neutron activation analysis. In: Kharfi F (ed) Imaging and radioanalytical techniques in interdisciplinary research – fundamentals and cutting edge applications. InTech, Rijeka Croatia

36. Shirai N, Hidaka Y, Yamaguchi A et al (2015) Neutron activation analysis of iron meteorites. J Radioanal Nucl Chem 303:1375–1380

37. Diaz O, Figueiredo A, Nogueira C et al (2005) Epithermal neutron flux characterization of the IEA-R1 research reactor, Sao Paulo, Brazil. J Radioanal Nucl Chem 266:153–157

38. ISO 13528:2022 (2022) Statistical methods for use in proficiency testing by interlaboratory comparisons. International organization for standardization, Genève, Switzerland

39. Gusev S, Ryabev V, Vorobyov V et al (2004) OST 41–08–212–04 Industrial standard quality management of analytical work. Error guidelines for chemical analysis of mineral resources and precision classification of laboratory analytical techniques. Published by FSMC VIMS, Moscow (**(in Russian)**)

40. Silachyov IYu (2018) Determination of rare earths in uranium raw material by neutron activation analysis and X-ray fluorescence. News Acad Sci RK, Ser Chem Technol 429(3):28–38

41. Rudnick RL, Gao S (2014) Composition of the continental crust. In: Holland HD, Turekian KK (eds) Treatise on geochemistry, vol 4, 2nd edn. Elsevier, College Park